Serine 23 and 36 Phosphorylation of Caveolin-2 Is Differentially Regulated by Targeting to Lipid Raft/Caveolae and in Mitotic Endothelial Cells†

Grzegorz Sowa,*,‡ Leike Xie,‡ Li Xu,‖ and William C. Sessa‖

Department of Medical Pharmacology and Physiology, University of Missouri, Columbia, Missouri 65212, and Department of Pharmacology, Vascular Cell Signaling and Therapeutics Program, Boyer Center for Molecular Medicine, Yale University School of Medicine, 295 Congress Avenue, New Haven, Connecticut 06536

Received August 22, 2007; Revised Manuscript Received November 1, 2007

ABSTRACT: In the present study, using a combination of reconstituted systems and endothelial cells endogenously expressing caveolins, we show that phosphorylation of caveolin-2 at serines 23 and 36 can be differentially regulated by caveolin-1 mediated subcellular targeting to lipid raft/caveolae and in endothelial cells synchronized in mitosis. Detergent insolubility and sucrose flotation gradient experiments revealed that serine 23 phosphorylation of caveolin-2 preferably occurs in detergent-resistant membranes (DRMs), while serine 36 phosphorylation takes place in non-DRMs. Furthermore, immunofluorescence microscopy studies determined that in the presence of caveolin-1, serine 23-phosphorylated caveolin-2 mostly localizes to plasma membrane, while serine 36-phosphorylated caveolin-2 primarily resides in intracellular compartments. To directly address the role of caveolin-1 in regulating phosphorylation of endogenous caveolin-2, we have used the siRNA approach. The specific knockdown of caveolin-1 in endothelial cells decreases caveolin-2 phosphorylation at serine 23 but not at serine 36. Thus, upregulation of serine 23 phosphorylation of caveolin-2 depends on caveolin-1-driven targeting to plasma membrane lipid rafts and caveolae. Interestingly, although serine 36 phosphorylation does not seem to be regulated in endothelial cells by caveolin-1, it can be selectively upregulated in endothelial cells synchronized in mitosis. The latter data suggests a possible involvement of serine 36-phosphorylated caveolin-2 in modulating mitosis.

Caveolin proteins are key components of detergent-resistant membranes (DRMs),[11] including lipid rafts and caveolae (*1*). Caveolins have many important functions. In addition to being key structural proteins that organize caveolae, caveolin proteins are important in regulating endocytosis and various aspects of cell signaling (*2, 3*). The caveolin family consists of three integral membrane proteins (*2*). Caveolin-1 and -2 (Cav-1 and Cav-2) are coexpressed on most cell types. A majority of the research on caveolin proteins have focused on the functions of Cav-1. Although Cav-1 has been extensively studied, very little is known about the function of Cav-2. Cav-2 interacts with Cav-1 to form a heterooligomeric complex within lipid rafts (*4, 5*). Interaction with Cav-1 is required to transport Cav-2 to the cell surface (*6, 7*). In the absence of Cav-1, Cav-2 is degraded, and its expression is markedly decreased (*8, 9*). Thus, it is possible that many of the functions previously attributed to Cav-1 may be due to modulation of Cav-1 function by Cav-2.

Caveolins are essential for caveolar biogenesis and function. Depending on the cell type, Cav-1 or Cav-3 expression is critical for the formation of caveolae (*8*−*10*).

Unlike the essential role for Cav-1 in caveolae assembly in nonmuscle cells and the respective role of Cav-3 in muscle cells, the role of Cav-2 is less clear. Caveolae are still present in ultrathin sections from lung capillary endothelium and in perigonadal adipose tissue of Cav-2 null mice, suggesting that Cav-2 is not necessary for caveolae formation at least in the examined tissues (*11*). However, it is uncertain if the absolute number of caveolae in Cav-2 null mice remains the same as in wild type mice, since quantitative analysis of caveolae number has not been performed. Also, it is unknown if the function of such Cav-2-depleted caveolae remains the same. Furthermore, interpretations of such knockout studies are complicated due to the possible compensatory mechanisms taking place during development. In contrast to the observations made in Cav-2 KO mice, there are several studies independently pointing at the supportive role of Cav-2 in the caveolae assembly in epithelial cells. The first evidence favoring the role of Cav-2 in caveolae assembly was made by Scheiffele et al., 1998 (*12*) using immunogold labeling followed by electron microscopy, observed that in the polarized epithelial cell line MDCK, Cav-1 and -2 are found together on basolateral caveolae whereas the apical mem-

† This work was supported by the Scientist Development Grant from National Center of the American Heart Association (0335028N to G.S.) and grants from the National Institute of Health (R01 HL64793, RO1 HL 61371, R01 HL 57665, PO1 HL 70295, Contract No. N01-HV-28186 (NHLBI-Yale Proteomics Contract) to W.C.S).

* Address correspondence to Grzegorz Sowa, 1 Hospital Drive, Rm. MA 415, Columbia, MO 65212, Tel. (573) 884-3188; Fax. (573) 884-4276; E-Mail: (sowag@health.missouri.edu).

‡ University of Missouri.

‖ Yale University School of Medicine.

[1] Abbreviations: DRMs, detergent-resistant membranes; Cav-1, caveolin-1; Cav-2, caveolin-2; CK2, casein kinase 2; HUVEC, human umbilical vein endothelial cells, FRT, fisher rat thyroid cells; TX-100, Triton X-100; CIP, calf intestinal phosphatase; siRNA, small interfering RNA.

10.1021/bi701709s CCC: $40.75
Published on Web 12/15/2007

brane, where only Cav-1 is present, lacks caveolae organelles. This observation suggests that Cav-1 and -2 heterooligomers, but not Cav-1 homooligomers, are involved in caveolar biogenesis in MDCK cells. A followup study on MDCK cells revealed that expression of a caveolin mutant which prevented the formation of the large Cav-1/-2 heterooligomeric complexes, led to intracellular retention of Cav-2 and disappearance of caveolae, while overexpression of wild type Cav-2 resulted in an increased number of caveolae, thus supporting the role of Cav-2 in caveolar biogenesis (*13*). Independently, using freeze-fracture immunoelectron microscopy, Fujimoto and colleagues (*14*) have shown that coexpression of Cav-1 and Cav-2 caused more efficient formation of deep caveolae than Cav-1 alone in hepatocellular carcinoma cell line (HepG2) lacking endogenous caveolins.

Recently, using electron microscopy of fixed cells, we have demonstrated that in addition to Cav-1, Cav-2 is necessary for de novo assembly of caveolae in the human prostate cancer cell line LNCaP (*5*). More importantly, the stimulatory effect of Cav-2- on Cav-1-dependent caveolae assembly in LNCaP cells involves the constitutive phosphorylation of Cav-2 at serines 23 and 36 by casein kinase 2 or a casein kinase 2-like kinase. Mutation of these residues reduced the stimulatory effect of Cav-2 on caveolae assembly, suggesting that serine phosphorylation of Cav-2 may regulate this process. Nothing is known about regulation of Cav-2 phosphorylation. Since caveolins may exist in other subcellular compartments, for example, ER and lipid droplets (*15, 16*) or golgi (*6, 7*), it may be important to determine if Cav-2 phosphorylation depends on subcellular location. Furthermore, very little is known about possible function of Cav-2 phosphorylation besides regulating Cav-1-dependent caveolae assembly (*5*). For example, the major phenotype in Cav-2 KO mice is the hyperproliferation of endothelial and possibly other cell types in the lung (*11*), pointing at a possible role for Cav-2 in regulating cell proliferation or differentiation.

In the current study using a combination of various fractionation techniques, followed by immunobloting with phospho-specific antibodies as well as immunofluorescent labeling of fixed cells, we have determined that serine phosphorylation of ectopically expressed Cav-2 can be reciprocally regulated by Cav-1 and subcellular localization. More recently, using the siRNA approach we have knocked down Cav-1 in human endothelial cells and confirmed a positive role of Cav-1 in regulating serine 23 phosphorylation of endogenously expressed Cav-2. Finally, we have also determined that phosphorylation of endogenously expressed Cav-2 is upregulated at serine 36 but not 23 in endothelial cells synchronized in mitosis, suggesting a possible role of serine 36 phosphorylation of Cav-2 in regulating endothelial cell mitosis.

MATERIALS AND METHODS

Antibodies. Rabbit anti-p-Ser 23 and anti-p-Ser 36 Cav-2 antibodies were generated in our laboratory as previously described (*5*). Mouse anti-Cav-1, anti-Cav-2, anti-Hsp-90, anti-β-actin, and anti-flotillin-1 were from BD Transduction Labs. Mouse anti-p-Y 27 Cav-2 was from BD Pharmingen. Rabbit anti-p-Y 19 Cav-2 was from ABR-Affinity BioReagents. Rat anti-HA was from Covance. Rabbit anti-cyclin B1 was from Santa Cruz Biotech.

Cells/Cell Lines. LNCaP cells (ATCC) were cultured in RPMI medium containing penicillin (100 units/mL), streptomycin (100 μg/mL), and 10% (v/v) fetal bovine serum (FBS) (Life Technologies). Fischer rat thyroid (FRT) cells were cultured in Ham's F-12 Coon's modified media (Sigma) containing penicillin (100 units/mL) and streptomycin (100ug/mL) supplemented with 5% FBS (Life Technologies, Grand Island, NY). Human umbilical vein endothelial cells (HUVEC) were isolated by collagenase treatment and maintained in culture in complete M199 medium (GIBCO/BRL) with 20% FBS, endothelial cell growth factor, 100 units/mL penicillin, and 100 μg/mL streptomycin.

Construction of Adenoviral Vectors and Transduction of Cells with Adenoviruses. Recombinant adenoviruses containing the cDNA encoding myc-tagged Cav-1 (Adcav-1-myc) was generated as described (*17*). Adenoviral, myc-tagged Cav-2 (Adcav-2-myc) was obtained from Dr. Enrique Rodriquez-Boulan and was constructed as described (*6*).

Replication-deficient adenoviruses expressing HA-tagged S23A and S36A Cav-2 under the control of the cytomegalovirus (CMV) promoter were generated by subcloning PCR-generated cDNAs encoding appropriate HA-tagged mutants of Cav-2 into pShuttle-CMV and then recombined with pAdEasy-1 by electroporation into BJ5183 *Escherichia coli* (Stratagene, La Jolla, CA). The recombinant adenoviral vector DNA was transfected into human embryonic kidney 293 cells with LipofectAMINE (Invitrogen), and the viruses were serially amplified in 293 cells, purified on a CsCl density gradient by ultracentrifugation, and titered using a cytopathic effect (CPE).

Transduction with Adenoviruses. For adenoviral transduction of cells, 2 days after plating, cells were infected with appropriate adenoviruses in serum free RPMI medium for 4 h. Adcav-1 and Adcav-2 were used at multiplicity of infection (MOI) of 5 for infection of LNCaP cells. Adcav-2 was applied at 20 MOI to infect FRT cells. β-Galactosidase in adenovirus (Ad-β-gal) was used at corresponding MOI to control for any changes in the cells caused by adenoviral infection itself. The viruses were removed after 4 h, and cells were left to recover for 48 h in complete media before all experiments. Preliminary experiments with cells infected with either Adcav-1 or Adcav-2 showed that nearly 100% of cells were Cav-1 or 2 positive, as assessed by immunofluorescence labeling using Cav-1 and Cav-2 antibodies (not shown).

Western Blot Analysis. Cells were lysed in a RIPA lysis buffer containing: 50 mM Tris HCl, 0.1 mM EGTA, 0.1 mM EDTA, 100 mM leupeptin, 1 mM phenylmethylsulfonyl fluoride, 1% (vol/vol) NP-40, 0.1% SDS, and 0.5% deoxycholic acid; pH 7.4, homogenized, and centrifuged for 10 min at 14 000 rpm and at 4 °C. Insoluble material was removed, and the supernatants were then mixed with Laemmli SDS loading buffer and boiled. An equal protein amount was loaded on 13% SDS-PAGE, and proteins were electroblotted onto nitrocellulose membranes. The membranes were washed in Tris-buffered saline with 0.1% Tween, blocked in 5% milk, and incubated with the appropriate primary antibodies, followed by incubation with fluorescently conjugated secondary antibodies (LI-COR Biotechnology). Bands were visualized using the Odyssey Infrared Imaging System (LI-COR Biotechnology).

Quantitation of Serine Phosphorylation of Caveolin-2. Cav-2 phosphorylation at serine 23 and 36 was quantified

using the Odyssey Infrared Imaging System (LI-COR Biotechnology). Unlike chemiluminescence used by the traditional Western blot, the Odyssey system is based on fluorescence signal, has at least 1 order of magnitude wider linear range of signal intensity, and thus proved to be more suitable for a quantitative Western blot. Unless otherwise stated the data is expressed as the densitometric ratio of P-Ser 23 or P-Ser 36 to total Cav-2 from one representative out of 3−4 total experiments.

Triton X-100 Insolubility Assay. Cells were lysed with 1% Triton X-100 in MBS (pH 6.5), and lysates were incubated for 10 min on ice and centrifuged at 48 000 g at 4 °C for 30 min. The supernatant was collected and considered as the Triton X-100 soluble fraction, while the Triton X-100 insoluble pellet was solubilized with an equal volume of SDS-PAGE loading buffer. Equal volumes of both samples were loaded on SDS-PAGE gel and western blotted.

Sucrose Fractionation of Low-Density Triton X-100 Insoluble Membrane Domains. Low density, Triton X-100-insoluble membrane domains were purified from cultured cells as follows. Cells were washed with ice cold MBS buffer, scraped, pelleted by centrifugation at 1000*g*, and lysed with 1% Triton X-100 in MBS containing proteases inhibitors. Homogenization was carried out with 10 strokes of a loosely fitting Dounce homogenizer. A 1 mL amount of the homogenate was adjusted to 42.5% sucrose and 0.5% TX-100 by the addition of 1 mL of 85% sucrose prepared in MBS, placed at the bottom of an ultracentrifuge tube, overlaid with 8 mL of 35% sucrose, topped with 2 mL of 15% sucrose (in MBS without TX-100), and centrifuged at 35 000 rpm for 20 h in an SW41 rotor (Beckman Instruments). A light scattering band confined to the 35−15% sucrose region was observed that contained flotilin-1 but excluded most other cellular proteins such as Hsp90. From the top of each gradient, 1 mL gradient fractions were collected to yield a total of 12 fractions. An equal volume from each gradient fraction was separated by a 13% SDS-PAGE and subjected to immunoblot analysis.

Velocity Sedimentation Gradients. Samples were dissociated by incubation with 500 μL of Mes-buffered saline, containing 25 mM Mes, pH 6.5, and 150 mM NaCl (MBS) plus 60 mM n-octyl-β-d-glucopyranoside (octyl glucoside). Solubilized material was then incubated in the absence of presence of CIP (U/mL) for 30 min at 37 °C, loaded atop a 5−50% linear sucrose gradient (4.3 mL), and centrifuged at 42 000 rpm for 16 h in a SW-50 rotor (Beckman Instruments, Palo Alto, CA). After centrifugation, nine gradient fractions were collected from the top mixed with SDS-PAGE loading buffer, and equal volumes were loaded, run on the 13% SDS-PAGE, and western blotted. Molecular mass standards for velocity gradient centrifugation were as follows: carbonic anhydrase (29 kDa), bovine serum albumin (BSA; 66 kDa), β-amylase (200 kDa), and apoferritin (443 kDa).

Immunofluorescence Labeling. Cells were processed for immunofluorescence as follows: cells were fixed with 3% paraformaldehyde in Dulbecco's phosphate-buffered saline, pH 7.4 (DPBS), for 15 min, and washed three times with DPBS. The residual aldehyde groups were quenched with 25 mM NH_4Cl in DPBS for 10 min. Cells were then incubated sequentially with 0.1% Triton X-100 (v/v) in DPBS for 10 min, DPBS plus 5% goat serum for 30 min, and thereafter with appropriate antibodies in 0.2% BSA for 2 h, washed three times, and incubated with fluorescein isothiocyanate- or Texas Red-labeled secondary antibodies (Jackson Immunoresearch Laboratories, West Grove, PA) diluted 1:500. Slides were mounted with Slowfade (Molecular Probes, Inc., Eugene, OR), and cells were observed and analyzed with a Zeiss Axiovert epifluorescence microscope OPENLAB software (Improvision, Lexington, MA).

siRNA Knockdown of Endogenous Cav-1 in Endothelial Cells. Smart pool containing siCONTROL Non-Targeting siRNA Pool #1 and Cav-1 siRNA were obtained from Dharmacon. Briefly, HUVEC were transfected with 10 nM of control and Cav-1 siRNA using oligofectamine according to manufacturer's protocol. Three days later, cells were lysed using RIPA buffer and lysates processed for Western Blot.

Cell Cycle Synchronization in Mitosis for Flow Cytometry and Western Blot. HUVEC were treated with 100 nM nocodazole for 16 h, and mitotic cells were collected by shake-off. For flow cytometry, cells were fixed and stained with 25 μg/mL propidium iodide (PI; Molecular Probes, Eugene, OR) and then subjected to analytic flow cytometry using a FACSort (BD Biosciences, Mountain View, CA). For Western Blot, mitotic cells were lysed with RIPA buffer and analyzed using appropriate antibodies against caveolins and mitotic marker protein, cyclin B1.

Pervanadate Treatment for Detecting Tyrosine Phosphorylation of Cav-2. HUVEC were incubated with 50 μM of freshly prepared pervanadate for 30 min, lysed with RIPA buffer, and processed for Western Blot with p-Y 19 and 27 Cav-2.

RESULTS

Cav-1 Upregulates Serine 23 and Downregulates Serine 36 Phosphorylation of Cav-2. To determine the relative level of Cav-2 phosphorylation in the absence or presence of Cav-1, we have transduced LNCaP cells with adenoviruses encoding Cav-2 that is epitope tagged with the myc antigen (Cav2-myc) (Figure 1A, lane 2) or a combination of Cav2-myc and Cav1-myc (lane 3). For comparison, we have also used lysates from HUVEC endogenously expressing both caveolins (lane 4). Coexpression of Cav-1 increased by up to 3-fold the densitometric ratio of P-Ser 23/Cav-2 (Figure 1A, bottom graphic panel, white bars) and decreased by 2-fold the respective ratio of P-Ser 36/Cav-2 (gray bars) relative to LNCaP lysates negative in Cav-1. Consistent with LNCaP coexpressing Cav-2 and -1, the P-Ser 23/Cav-2 ratio was ca. 7-fold higher and the respective ratio of P-Ser 36/Cav-2 was ca. 1.5-fold lower in HUVEC (lane 4) relative to LNCaP cells with Cav-2 alone. To determine if the observed reciprocal regulation of Cav-2 serine phosphorylation by Cav-1 is a more general phenomenon, we have used FRT cells. These cells express Cav-2 but not Cav-1 (Figure 1B, lane 1). Our phospho-serine specific antibodies against human Cav-2 did not detect any P-Ser 23- or 36-Cav-2-specific signal, most likely because of differences between human and rat sequences or because the serine phosphorylation level of Cav-2 in these cells is below the detection limit. In this system, Cav-1-induced upregulation of P-Ser 23 was very high, i.e., ca. 8- to 10-fold at all time points after infection (Compare Figure 1B, lanes 2−5 vs 6−9 and the corresponding top graph representing P-Ser 23/Cav-2 ratio). Conversely, Cav-1-induced downregulation of P-Ser

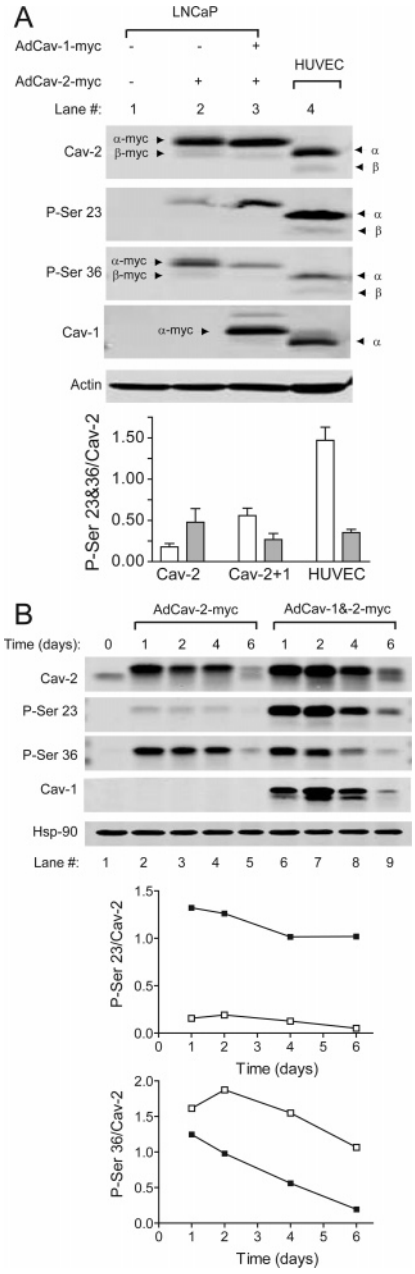

FIGURE 1: Reciprocal regulation of serine 23 and serine 36 phosphorylation of caveolin-2 by caveolin-1. A. Caveolin-1 (Cav-1) and -2 (Cav-2) negative LNCaP cells (lane 1) were infected with adenoviruses encoding myc-tagged caveolins (Cav-myc), i.e., Cav-2-myc (lane 2) or Cav-2-myc plus Cav-1-myc (lane 3). Two days after infection, cells were lysed and Western blotted with antibodies against Cav-2 and Cav-1, phosphoserine-specific antibodies against Cav-2 (P-Ser 23 and P-Ser 36), and actin (as a loading control). Symbols on the left: α- and *β*-myc stand for α- and *β*-isoforms of myc-tagged Cav-1 or -2. Lane 4 are lysates of HUVEC expressing endogenous caveolins. Symbols on the right: α and *β* stand for α- and *β*-isoforms of Cav-2 or -1. The bottom graph represents the mean ± SEM from three independent experiments of the densitometric ratios of P-Ser 23/Cav-2 (white bars) and P-Ser 36/Cav-2 (gray bars) in samples expressing Cav-2 (lanes 2−4). B. Parental FRT cells (lane 1) infected with Cav-2-myc adenovirus (AdCav-2-myc; lanes 2−5) or a combination of Cav-2 and -1-myc adenoviruses (AdCav-1- and -2-myc; lanes 6−9) were lysed at indicated time points and Western blotted as in A. The graphs represent the densitometric ratios of P-Ser 23 (upper graph) or P-Ser 36 (bottom graph) to Cav-2 plotted against time after completing the infection (days). Open squares represent samples expressing Cav-2-myc alone, while filled squares indicate samples coexpressing Cav-2- and -1-myc.

36 gradually increased with time after infection from ca. 1.3-fold to ca. 3-fold between the first and fourth day after adenoviral transduction (Figure 1B, bottom graph). Thus, in two distinct reconstitution cell systems, Cav-1 regulates Cav-2 serine phosphorylation.

The Reciprocal Regulation of Cav-2 Serine Phosphorylation by Cav-1 Is Proportional to the Degree of Insolubility of Cav-2 in Triton X-100. Several authors, including our group have shown that Cav-2 expressed alone is almost entirely soluble in TX-100, and that coexpression of Cav-1 renders Cav-2 mostly TX-100 insoluble. To determine how the observed effects of Cav-1 on Cav-2 serine phosphorylation influence Cav-2 TX-100 solubility, we coexpressed Cav-2- and -1-myc which yielded nearly equal amounts of total Cav-2 in TX-100 soluble and insoluble compartments in LNCaP cells (Figure 2A, top immunoblot, lanes 5 vs 6 and 2B, white bars). Interestingly, under the latter conditions, the ratio of P-Ser 23/Cav-2 was almost 2-fold higher in TX-100 insoluble than in TX-100 soluble fraction (second top immunoblot, lanes 5 vs 6; black bars). Conversely, P-Ser 36/Total Cav-2 was downregulated in TX-100 insoluble fraction (third immunoblot from the top, lanes 5 vs 6; gray bars). A comparable fold of upregulation of P-Ser 23 relative to total Cav-2 could be seen in TX-100 insoluble fractions from HUVEC lysates (Figure 2, lanes 7 vs 8). These data suggest that increased detergent insolubility of Cav-2 stimulated by coexpression of Cav-1 contributes to upregulation of serine phosphorylation of Cav-2.

Targeting to DRMs but Not Direct Interaction with Cav-1 Is Necessary for Reciprocal Regulation of Serine Phosphorylation of Cav-2. To determine the role of targeting to light buoyant density DRMs (containing lipid rafts and caveolae membranes), sucrose flotation gradients of cells lysed with TX-100 were used. Surprisingly, approximately 20% of Cav-2 expressed in the absence of Cav-1 was able to reach DRMs (Figure 3A, top panel, lanes 1−4). Interestingly, DRMs-associated Cav-2 was heavily phosphorylated at serine 23 (ca. 40% of P-Ser 23 in DRMs) and only lightly phosphorylated at serine 36 (ca. 10% of total P-Ser 36 in DRMs). As expected, coexpression of Cav-1 increased the levels of total Cav-2 and phosphorylated Cav-2 in DRMs (Figure 3B). These data suggest that targeting of Cav-2 to DRMs is a key mechanism of reciprocal regulation of Cav-2 serine phosphorylation by Cav-1. Finally, endogenously expressed Cav-2 in endothelial cells can be nearly entirely (95%) found in DRMs (Figure 3C) and thus explaining why the overall level of Cav-2 phosphorylation at serine 23 is very high while at serine 36 is very low.

Serine 23 Phosphorylation of Cav-2 Positively Correlates with Cav-1-Mediated Targeting of Cav-2 to Plasma Membrane, While Serine 36 Phosphorylation of Cav-2 Is More Limited to Intracellular Compartments. To further characterize the level of Cav-2 phosphorylation in different subcellular compartments, immunofluorescence microscopy of FRT cells was performed with P-Ser 23 and P-Ser 36 Cav-2 antibodies. FRT cells were adenovirally infected with HA-tagged wild type Cav-2 (Figure 4A, AdWTCav-2) or the phospho-mutant where the Serine 23 was mutated to alanine (S23A-Cav-2; AdS23ACav-2). As seen in Figure 4A, the anti-P-Ser 23 antibody labeled WT but not S23A-Cav-2, while anti-HA Ab labeled both, thus proving specificity of anti-P-Ser 23-Cav-2 antibody for immunofluorescence studies. The speci-

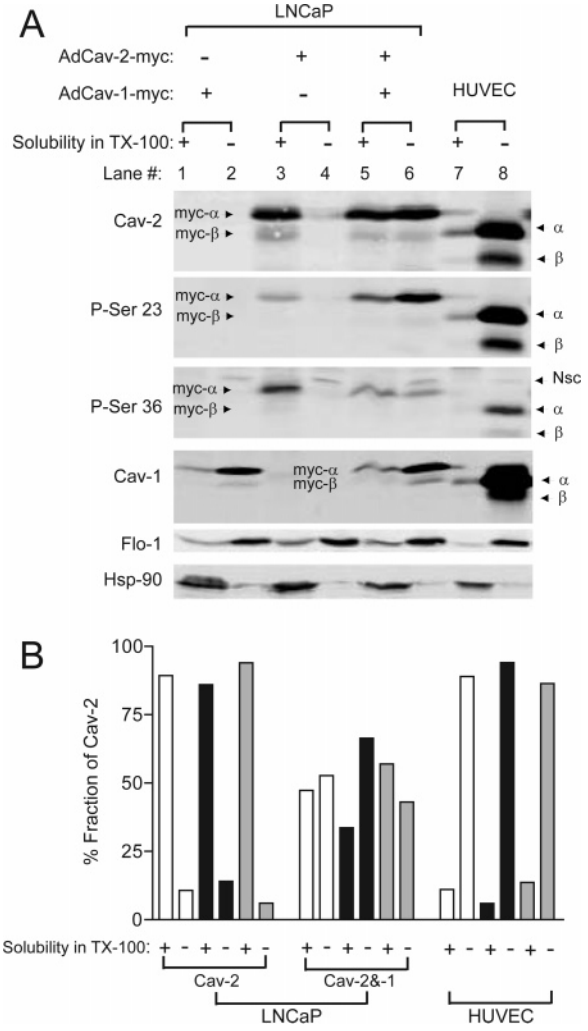

FIGURE 2: Caveolin-1-induced regulation of serine 23 and 36 phosphorylation positively correlates with insolubility of caveolin-2 in TX-100. A. LNCaP cells infected with adenoviruses encoding Cav-1-myc (lanes 1−2), Cav-2-myc (lanes 3−4), Cav-2- and -1-myc (lanes 5−6) or HUVEC expressing endogenous Cav-1 and -2 were lysed with 1% TX-100 in MBS buffer, pH 6.5, at 4 °C and TX-100-soluble (+) and -insoluble (−) fractions were Western blotted with indicated antibodies, i.e., Cav-1, Cav-2, Cav-2 phospho-specific antibodies against serine 23 (P-Ser 23) and 36 (P-Ser 36), flotillin-1 (Flo-1), and HSP-90. B. The relative distribution between TX-100-soluble (+) and -insoluble (−) fractions for total Cav-2 (white bars), P-Ser 23 (black bars), and P-Ser 36 (gray bars). Symbols on the left: α- and *β*-myc stand for α- and *β*-isoforms of myc-tagged Cav-1 or -2. Symbols on the right: α and *β* stand for α- and *β*-isoforms of Cav-2 or -1. NSC indicates nonspecific bands detected with P-Ser 36 Cav-2 antibody in TX-100-insoluble fractions.

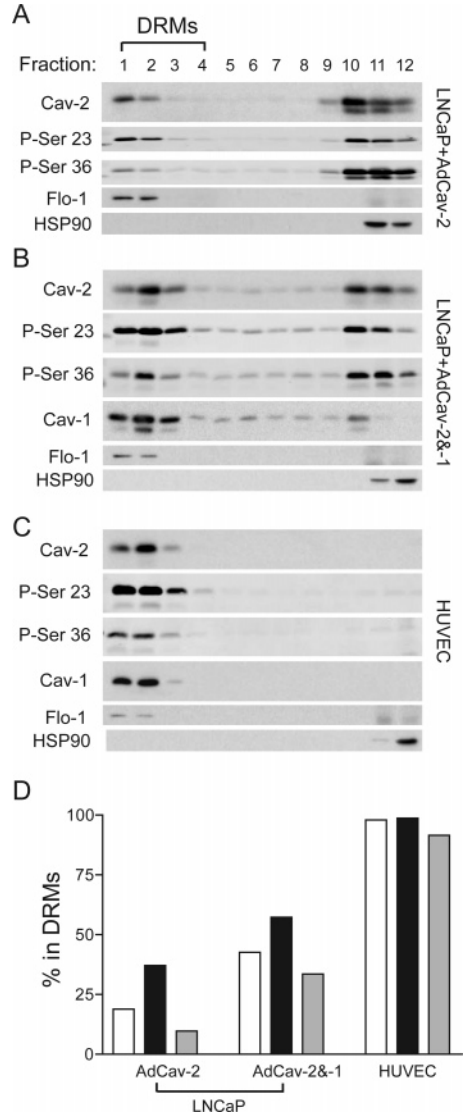

FIGURE 3: Caveolin-2 in detergent-resistant membranes (DRMs) exhibits reciprocal phosphorylation of serines 23 and 36. LNCaP cells infected with adenovirus encoding Cav-2 alone (Panel A), a combination of Cav-2 and Cav-1 (Panel B), or HUVEC expressing endogenous Cav-1 and -2 (Panel C) were lysed with 1% TX-100 in MBS buffer, pH 6.5, at 4 °C. Lysates were adjusted to 43.5% sucrose, overlaid with 35% and 10% sucrose, and centrifuged at 160 000 g for 20 h, and 12 × 1 mL fractions were collected from the top. All 12 fractions were Western blotted with the following antibodies: Cav-1, Cav-2, Cav-2 phospho-specific antibodies against serine 23 (P-Ser 23) and 36 (P-Ser 36), DRMs marker protein, flotillin-1 (Flo-1), and a cytosolic protein, HSP-90. In panel D, the % total Cav-2 (white bars), P-Ser 23 (black bars), and P-Ser 36 (gray bars) in DRMs from LNCaP cells expressing Cav-2 alone or Cav-2 and -1 or for HUVEC are shown.

ficity was further supported by the fact that incubation with 10× excess of phospho-peptide used to raise and purify P-Ser 23 Ab nearly completely abolished P-Ser 23 but not total Cav-2 staining in HUVEC (not shown). P-Ser 23 colocalized well with HA-specific signal in the perinuclear region of FRT cells expressing Cav-2-HA alone (depicted by arrowheads in top panel). Coexpression of Cav-1 (AdWTCav-2+1) redistributed majority of Cav-2 to the plasma membrane. Under these conditions, P-Ser 23 Cav-2 could preferably be detected in the plasma membrane (depicted by arrows in third panel) as a significant portion of Cav-2 remaining in perinuclear region was stained with anti-HA but not anti-P-Ser 23 antibody (depicted by arrowheads in third panel). Furthermore, this observation was confirmed in HUVEC in which majority P-Ser 23 signal could be found in plasma membrane (depicted by arrows in fourth panel), and there were also perinuclear dots selectively stained with anti-Cav-2 but not P-Ser 23 antibody (depicted by arrowheads in fourth panel). These data suggest that in cells expressing endogenous Cav-2 and -1, such as HUVEC, the phosphorylation of Cav-2 at serine 23 primarily occurs in the plasma membrane.

Cav-1 is essential for caveolae formation and thus is the best marker protein for caveolae localization. Therefore, to further determine that plasma membrane staining with P-Ser

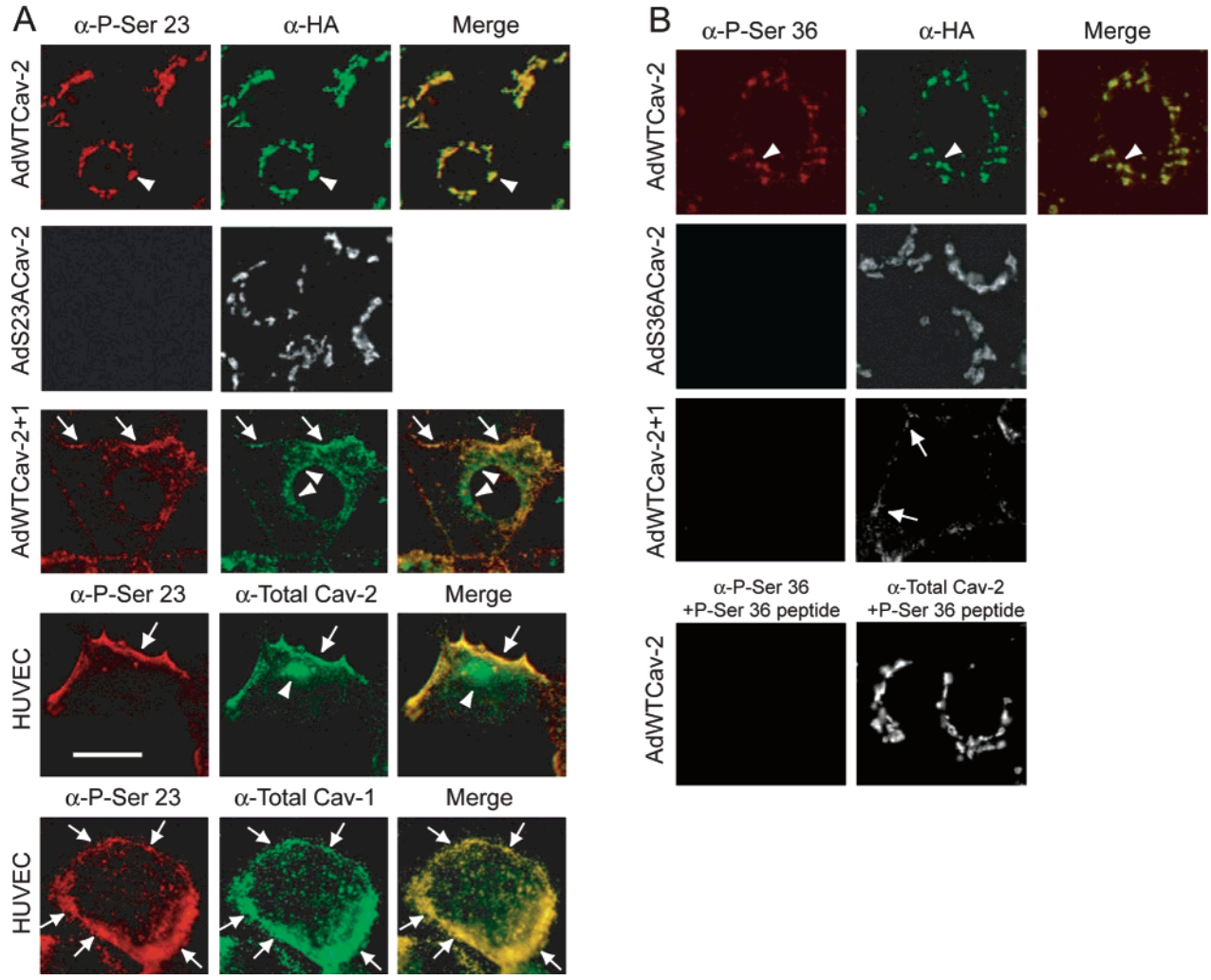

FIGURE 4: Preferable targeting of phospho-serine 23 caveolin-2 to plasma membrane and phospho-serine 36 caveolin-2 to intracellular compartments. A. In top three panels, FRT cells were infected with adenoviruses encoding HA-tagged WT caveolin-2 (AdWTCav-2), S23A Cav-2 (AdS23ACav-2), or WTCav-2 and -Cav-1 (AdWTCav-2+1), fixed and colabeled with α-P-Ser 23-Cav-2 (red images) and α-HA (green images) antibodies. In the fourth panel, HUVEC expressing endogenous Cav-1 and -2 were costained with α-P-Ser 23-Cav-2 (red image) and α-total Cav-2 (green image). In the bottom panel, HUVEC were costained with α-P-Ser 23-Cav-2 and α-Cav-1. Arrowheads in first (top) panel indicate perinuclear localization. Arrowheads in the third and fourth panels depict intracellular Cav-2 stained with α-HA or α-total Cav-2 but not α-P-Ser 23-Cav-2, while arrows in these panels indicate plasma membrane staining with all above-mentioned antibodies. Arrows in the bottom panel indicate plasma membrane-associated P-Ser 23 colocalizing with Cav-1. Scale bar: 20 μm. B. FRT cells were infected with adenoviruses encoding HA-tagged WT caveolin-2 (AdWTCav-2), S36A Cav-2 (AdS36ACav-2), or WTCav-2 and -Cav-1 (AdWTCav-2+1), fixed, and colabeled with α-P-Ser 36-Cav-2 and α-HA (top three panels) or α-P-Ser 36-Cav-2 and α-total Cav-2 (bottom panel). Arrowheads in AdWTCav-2 panel point at perinuclear staining with α-P-Ser 36 and α-HA. Arrows in AdWTCav-2+1 panel depict plasma membrane staining with α-HA. Bottom panel: FRT cells infected with AdWTCav-2 were costained with α-P-Ser 36-Cav-2 and α-total Cav-2 in the presence of 10× molar excess of peptide containing P-Ser 36, which was used to raise and purify α-P-Ser 36-Cav-2.

23 Ab is within caveolae, we performed colocalization studies with Cav-1 Ab (Figure 4A, bottom panel). Mostly plasma membrane located P-Ser 23 Cav-2 colocalized very well with Cav-1 in HUVEC expressing endogenous caveolins (Figure 4A, bottom panel, depicted by arrows). This data suggests that plasma membrane-associated serine 23 phosphorylation of Cav-2 is indeed localized to caveolae. Thus overall, our immunofluorescence data corresponds well with our sucrose fractionation findings, indicating that plasma membrane lipid raft/caveolae is the primary location for Cav-2 phosphorylation at serine 23 in cells coexpressing both caveolins.

Next, FRT cells were adenovirally infected with HA-tagged wild type Cav-2 (Figure 4B, AdWTCav-2) or the phospho-mutant where the serine 36 was mutated to alanine (S36A-Cav-2; AdS36ACav-2). Anti-P-Ser 36 antibody labeled WT but not S36A-Cav-2-expressing cells, while anti-HA stained both, thus proving the specificity of anti-P-Ser 36-Cav-2 antibody for immunofluorescence studies. Furthermore, co-incubation with 10-fold molar excess of the corresponding phospho-peptide used to raise and purify P-Ser 36-Cav-2 Ab abolished P-Ser 36- but not total Cav-2-specific fluorescent signal in FRT cells expressing human HA-tagged Cav-2 (Figure 4B, bottom panel). Interestingly, under conditions in which coexpression of Cav-1 in FRT cells resulted in nearly a complete redistribution of Cav-2 to plasma membrane (Figure 4B, third panel from the top), we were unable to detect P-Ser 36-specific signal. This suggests that Cav-1-driven redistribution of Cav-2 to plasma membrane caveolae may limit phosphorylation of serine 36. Because P-Ser 36 is closer to the domain interacting with Cav-1, it is possible that direct interaction of Cav-2 with Cav-1 and

embedding it into high molecular heterooligomeric complexes may compromise accessibility of this epitope for P-Ser 36 Ab in fixed cells. This could be also the case in HUVEC coexpressing endogenous caveolins in which we were unable to obtain satisfactory P-Ser 36-Cav-2 specific staining (not shown). In addition, the antibody appears to cross-react with unidentified protein(s) of nuclear origin in HUVEC (not shown), precluding the use of this antibody for immunofluorescent labeling of HUVEC and probably other human cell types.

Cav-2 Oligomerization with Cav-1 Limits Ability of Calf Intestinal Phosphatase to Dephosphorylate Phospho-serine Residues of Cav-2. To determine the role of Cav-1 in stabilizing phospho-serines 23 and 36 of Cav-2, we tested potential resistance of phospho-Cav-2 to dephosphorylation by the broad spectrum phosphatase, calf intestinal phosphatase (CIP). Treatment of lysates from Cav-2 expressing LNCaP cells with CIP in the absence of phosphatase inhibitors yielded a complete loss of the phospho-specific signal at both serine residues (Figure 5A, compare lanes 1 and 2 in first and second panels from the top). In contrast to cells expressing Cav-2 alone, there was only partial loss of phospho-specific signal upon treatment of lysates from Cav-2 and -1 coexpressing cells with CIP (lane 3 vs 4). CIP was also partially effective in lysates from HUVEC coexpressing endogenous caveolins-1 and -2 (lane 7 vs 8). Moreover, protein denaturation by boiling of the lysates in the presence of 1% sodium dodecyl sulfate (SDS) and diluting the SDS 10-fold with a buffer containing 1% NP40/0.1% SDS prior to treatment with CIP increased the efficiency of dephosphorylating Cav-2 at both sites (lanes 5 vs 6 for LNCaP and lanes 9 vs 10 for HUVEC lysates).

Because the latter data suggested that formation of high molecular weight heterooligomers with Cav-1 could play a role in the observed partial protection from CIP-mediated dephosphorylation of Cav-2, we performed velocity sedimentation gradient on lysates from LNCaP coexpressing Cav-2 and -1, preincubated in the absence (-) or presence of CIP (+) at 37 °C for 30 min (Figure 5B). This molecular weight-based sedimentation assay revealed that CIP preferably removes phosphates from monomeric and dimeric Cav-2 but not from Cav-2 engaged by Cav-1 in high molecular weight heterooligomeric complexes. Overall, this data suggests that oligomerization with Cav-1 can potentially limit serine dephosphorylation of Cav-2 by cellular phosphatases.

Serine 23 Phosphorylation of Endogenously Expressed Cav-2 Is Downregulated by a Specific Knockdown of Cav-1 in Endothelial Cells. To verify if reciprocal regulation of Cav-2 phosphorylation by Cav-1 also occurs in cells expressing endogenous Cav-2, we used the siRNA approach. More specifically, acute >70% knockdown of endogenous Cav-1 in HUVEC, which did not affect expression of Cav-2 within the 72 h time frame after transfection (Figure 6A, Cav-1 and -2 immunoblots, lane 2 vs 1, Figure 6B, top graph), reduced by >50% the P-Ser 23 Cav-2 specific signal (Figure 6A, P-Ser 23 immunoblot, lane 2 vs 1, Figure 6B, bottom graph). Interestingly, Cav-1 knockdown did not affect the P-Ser 36 specific signal (Figure 6A, P-Ser 36 immunoblot, lane 2 vs 1, Figure 6B, bottom graph). Unlike serine phosphorylation, using phospho-specific antibodies against tyrosine 19 and 27 phosphorylated Cav-2, we were unable to detect tyrosine phosphorylation of Cav-2 in lysates from HUVEC treated

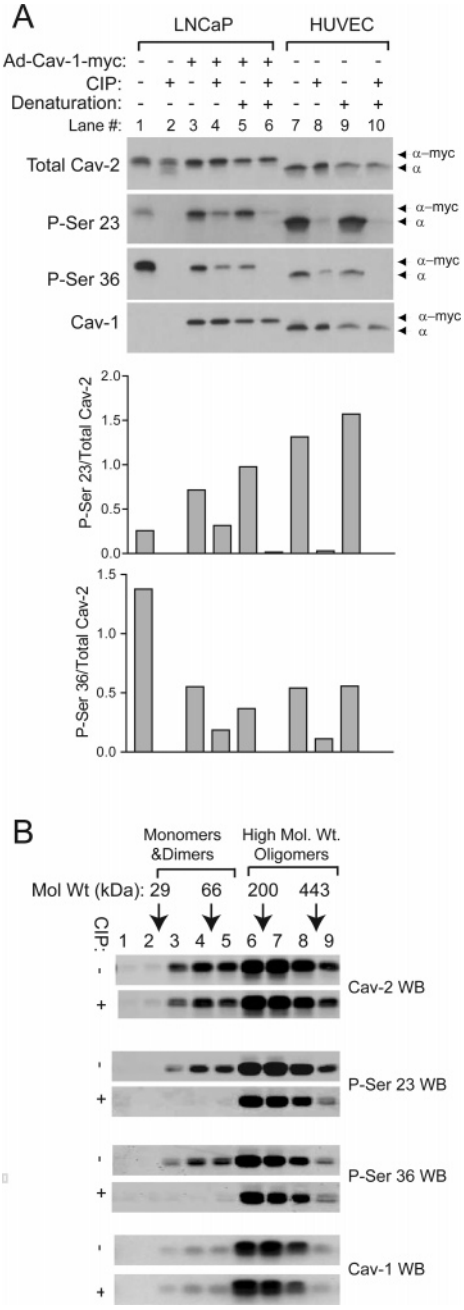

FIGURE 5: Oligomerization of caveolin-1 with caveolin-2 protects against phosphatase-mediated serine dephosphorylation of caveolin-2. A. Lysates of LNCaP cells infected with adenoviruses expressing myc-tagged caveolins, i.e., Cav-2-myc alone (lanes 1−2), coexpressing Cav-2-myc and -1-myc (lanes 3−6) and HUVEC expressing endogenous Cav-2 and -1 (lanes 7−10) were treated for 30 min in the absence (lanes 1, 3, 5, 7, and 9) or in the presence of calf intestinal phosphatase CIP (lanes 2, 4, 6, 8, and 10). In addition, lysates from LNCaP coexpressing Cav-2 and -1-myc (lanes 5 and 6) and those of HUVEC (lanes 9 and 10) were incubated in the presence of 1% SDS at 100 °C for 10 min prior to treatment with CIP. Lysates were Western blotted with indicated antibodies, i.e., total Cav-2, phospho-specific antibodies against Cav-2 at serine 23 (P-Ser 23) and 36 (P-Ser 36), and Cav-1 antibody. The top graph represents the densitometric ratios of P-Ser 23/Cav2 and the bottom graph P-Ser 36/Cav2 for each lane. Arrows with associated symbols α-myc point at α-isoform of Cav-2-myc or Cav-1-myc while arrows with α indicate α-isoform of wild type Cav-2 and -1. B. Lysates of LNCaP coexpressing Cav-2-myc and Cav-1-myc fractionated in a high-speed sedimentation gradient were treated for 30 min in the absence (−) or in the presence of CIP (+), and Western blotted as in A.

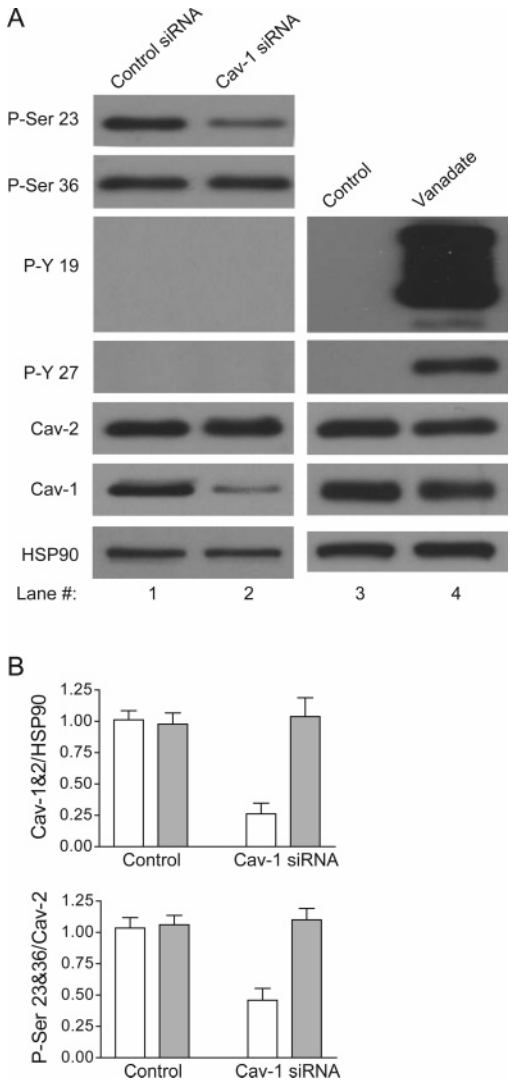

FIGURE 6: Specific knockdown of caveolin-1 with siRNA down-regulates serine 23 but not serine 36 phosphorylation of caveolin-2. A. Immunoblots: lanes 1 and 2: HUVEC were transfected with control and caveolin-1 (Cav-1) siRNA using oligofectamine. Three days after transfection, cells were lysed using RIPA buffer and processed for Western blot with indicated antibodies against phosphorylated Cav-2 at serine 23 (P-Ser 23) and serine 36 (P-Ser 36), at tyrosine 19 (P-Y 19) and tyrosine 27 (P-Y 27), and total Cav-2, Cav-1, and HSP90. The graphs represent mean densitometric ratios ± SEM from three independent experiments. Lanes 3 and 4: control HUVEC or treated with 50uM sodium pervanadate (Vanadate) for 30 min, followed by lysis and Western blotting with antibodies against Cav-2 phosphorylated at tyrosine 19 (P-Y 19) and tyrosine 27 (P-Y 27), and total Cav-2, Cav-1, and HSP-90. B. Quantitative analysis of data from immunoblots (lanes 1 and 2): Top graph shows densitometric ratio of Cav-1 (white bars) or Cav-2 (gray bars) to HSP90. Bottom graph represents densitometric ratio of P-Ser 23- (white bars) or P-Ser 36-Cav-2 to total Cav-2.

with control or Cav-1 siRNA (Figure 6A, P-Y 19 and 27 immunoblots, lanes 1 and 2). As a positive control, treatment with tyrosine phosphatase inhibitor pervanadate at 50 μM resulted in a robust phosphorylation of tyrosine 19 and a moderate phosphorylation of tyrosine 27 (Figure 6A, PY 19 and 27 immunoblots, lane 4).

Serine 36 but Not 23 Phosphorylation of Endogenously Expressed Cav-2 is Upregulated in Endothelial Cells Synchronized in Mitosis. Because of the hyperproliferative phenotype in the lung of Cav-2 KO mice (*11*), suggesting a potential role for Cav-2 in regulating cell growth/differentiation, we were curious if serine or tyrossine phosphorylation could be modulated during various phases of cell cycle. For this reason, we have synchronized HUVEC in different phases of cell cycle and looked at serine and tyrosine phosphorylation of Cav-2. Neither Go/G1 synchronization by serum starvation nor double thymidine synchronization at G/S yielded any significant changes in serine phosphorylation of Cav-2, relative to asynchronous cells (not shown). However, in HUVEC synchronized in mitosis, there was ca. 2.5-fold increase in serine 36 phosphorylation of Cav-2 relative to asynchronous cells (Figure 7). Conversely, relative serine 23 phosphorylation of Cav-2 was only negligibly lower in mitotic cells. Using p-Y 19 and 27-Cav-2 antibodies, we have also examined potential changes in tyrosine phosphorylation on Cav-2 but failed to detect it under any of above-described conditions (not shown).

DISCUSSION

Previously, we have shown that ectopically expressed Cav-2 in LNCaP cells can be serine phosphorylated at the two N-terminal serine residues 23 and 36 and thereby regulate the ratio of plasma membrane caveolae and plasma membrane vesicle numbers in human prostate cancer cells LNCaP (*5*). In the current study, using two reconstituted systems (LNCaP and FRT cells) and human endothelial cells endogenously expressing both Cav-1 and -2, we demonstrate that the serine phosphorylation of Cav-2 serine is reciprocally regulated by Cav-1-induced translocation of Cav-2 from detergent-soluble perinuclear compartments to detergent-resistant plasma membrane lipid rafts and caveolae. The stimulating effect of Cav-1 on serine 23 phosphorylation of Cav-2 in LNCaP and FRT cells is consistent with our data in HUVEC expressing both caveolins. Furthermore, using siRNA against Cav-1, we confirm the specific role of Cav-1 in upregulating serine 23 phosphorylation of endogenous Cav-2 in endothelial cells. Finally, we also show an example of selective upregulation of serine 36 phosphorylation in endothelial cells synchronized in mitosis.

The reciprocal effect of Cav-1 on serine phosphorylation of Cav-2 appears to be solely based on translocation of detergent soluble perinuclear Cav-2 to detergent-insoluble plasma membrane caveolae and lipid rafts but not due to conformational changes of Cav-2 resulting from its interaction with Cav-1. This conclusion is supported by the observation showing that a small fraction of Cav-2 expressed in LNCaP cells is able to reach DRMs and is serine phosphorylated in a manner similar to HUVEC endogenously expressing Cav-2 and -1., i.e., the Cav-2 associated with DRMs in both cases displays high phosphorylation at serine 23 and reduced phosphorylation at serine 36. Moreover, by microscopy, the enriched P-Ser 23 Cav-2 in plasma membrane correlates with its TX-100 insolubility and the subsequent flotation in sucrose gradient data.

In light of our findings we surmise two potential scenarios for serine phosphorylation of Cav-2 expressed in the absence or in the presence of Cav-1. i. Cav-2 expressed in the absence of Cav-1 is mostly retained in the TX-100-soluble, perinuclear Golgi region of cells (*6*) where it is primarily phosphorylated at serine 36 and to a lesser extent on serine 23 (see Figures 2-4). ii. Coexpression with Cav-1 dramatically shortens the time that Cav-2 is present in the Golgi

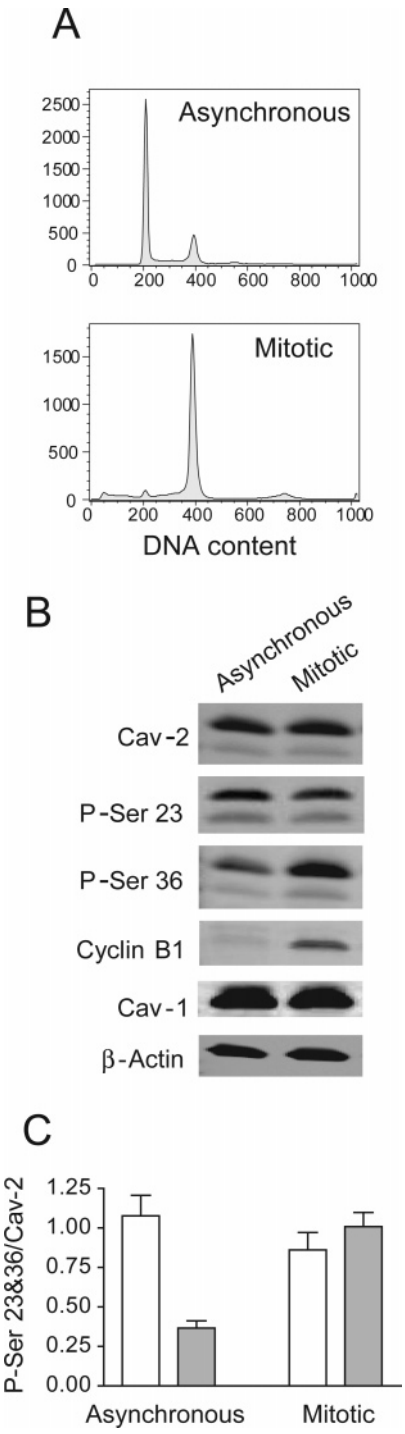

FIGURE 7: Phosphorylation of serine 36 but not serine 23 of caveolin-2 is upregulated in endothelial cells synchronized in mitosis. Control (asynchronous) and synchronized in mitosis upon treatment with 100 nM nocodazole for 16 h and shake-off (mitotic) HUVEC were processed for flow cytometry (A) or Western blot (B). A: DNA content from control/asynchronous (top) and synchronized in mitosis cells (bottom) measured in a linear scale. B: Western blot evaluation with phospho-serine 23 (P-Ser 23) and 36 (P-Ser 36) and total caveolin-2 (Cav-2) and Cav-1, as well as mitotic cyclin B1 antibodies. C: Densitometric ratio of P-Ser 23 (blank bars) and P-Ser 36 (dotted bars) to total Cav-2 representing mean ± SEM from three experiments.

and thus limits serine 36 phosphorylation, while allowing Cav-2 to reach plasma membrane caveolae where serine 23 phosphorylation is preferred. The latter conclusion is strongly supported by the fact that P-Ser 23 is mostly located to plasma membrane regions of FRT cells (infected with AdCav-1 and -2) and HUVEC endogenously expressing Cav-1 and -2. Finally, acute knockdown of endogenous Cav-1 in HUVEC results in specific downregulation of P-Ser 23 but not P-Ser 36-Cav-2, proving that serine 23 phosphorylation of endogenous Cav-2 depends on Cav-1.

Our data and conclusions using human Cav-2 are in an excellent agreement with the work of Scheiffelle et al. (*12*), who observed location-dependent basal phosphorylation of canine Cav-2. However, these authors did not examine the specific phosphorylation sites and kinase. Previously, we have provided several pieces of evidence suggesting that CK2 or CK2-like kinase is involved in Cav-2 serine phosphorylation (*5*). Although CK2 is primarily located to the nucleus and cytosol (*18*), it has also been shown to be present in the Golgi itself (*19*) or to be recruited to plasma membrane via its pleckstrin homology domain (*20*). It is uncertain why serine 36 is primarily phosphorylated in the perinuclear region while serine 23 is primarily phosphorylated in the plasma membrane region. Most likely this differential serine phosphorylation of Cav-2 is the result of preferential access of either serine residue to cytosolic, Golgi-, and potentially plasma membrane-associated CK2/CK2-like kinase(s). For example, the structural conformation of Cav-2 within the Golgi membranes could favor serine 36 phosphorylation by Golgi-associated CK2. This scenario could reverse once Cav-2 leaves the Golgi and reaches plasma membrane rafts/caveolae where a cholesterol/lipid-rich environment may prevent serine 36 from being phosphorylated by CK2. At the same time, serine 23 could be efficiently phosphorylated by cytosolic and possibly plasma membrane-associated CK2. Furthermore, high molecular heterooligomeric complexes with Cav-1 along with the cholesterol/lipid-rich environment of caveolae may to some degree prevent P-Ser 23 dephosphorylation by endogenous phosphatases and thus further contribute to the elevated phosphorylation state of serine 23 in plasma membrane caveolae compared to the Golgi.

It is important to reconcile our new findings showing regulation of serine phosphorylation of Cav-2 with the previously observed regulatory role of Cav-2 in determining the number of plasma membrane versus subplasmalemmal caveolae (*5*). Our previous data suggested that serine 36 is more critical than serine 23 for caveolae assembly. Serine 36 is poorly phosphorylated relative to serine 23 in cells endogenously coexpressing both caveolins such as HUVEC. Although our immunofluorescent labeling did not detect a significant amount of P-Ser 36 Cav-2 in plasma membrane of FRT cells coexpressing both caveolins, it is very likely that the overall weak signal for this P-Ser 36 antibody may account for this. In addition, although the P-Ser 36 antibody was specific for this residue in Western blots, the same antibody-labeled nuclei in fixed HUVEC did not permit analysis of its subcellular location in the latter cells. However, sucrose gradient fractionation clearly demonstrated that Cav-2 present in DRMs of HUVEC is phosphorylated at serine 36, suggesting that the low level of Cav-2 phosphorylation at serine 36 is sufficient for its role in caveolae biogenesis and assembly. This conclusion is supported by data showing that high molecular weight heterooligomers of Cav-1 and -2 (containing 14−16 molecules of each caveolin (*12*, *21*)) are believed to initiate caveolae assembly.

Our data suggest at least one or more of the Cav-2 molecules engaged in heterooligomer assembly is phosphorylated at serine 36 and that multiple heterooligomeric structures containing serine 36 phosphorylated Cav-2 are required to assemble a single invaginated caveola.

Previously, we have shown that serine 23 phosphorylation does not affect caveolae assembly per se, but it cooperates with serine 36 during caveolae biogenesis and may affect the ratio of caveolae to subplasmalemmal vesicles. Thus, by reconciling the latter observations with the results showing that serine 23 is robustly phosphorylated in plasma membrane caveolae, one could hypothesize that serine 23 phosphorylation/dephosphorylation may be involved in regulating caveolae/vesicle turnover and possibly be implicated in caveolae-mediated transport.

Our data showing a selective increase in serine 36 phosphorylation on Cav-2 endogenously expressed in endothelial cells synchronized in mitosis strongly suggest that serine 36 phosphorylation of Cav-2 could regulate cell cycle, in particular mitosis. Interestingly, the hyperproliferative phenotype involving increased number of endothelial cells in the lung of Cav-2 KO mice (*11*) strongly suggests that Cav-2 may regulate cell growth. The exact mechanism of the potential regulation of endothelial cell proliferation remains to be established, but serine 36 phosphorylation of Cav-2 may be involved in this process.

Considering that Cav-2 has been also reported to be phosphorylated on tyrosines 19 and 27 (*22*, *23*), using the phospho-specific antibodies to the latter sites, we have also examined tyrosine phosphorylation of Cav-2. Although, using immunoblotting of total cell lysates, we were able to detect both phospho-tyrosine phosphorylated Cav-2 in endothelial treated with general tyrosine phosphatase inhibitor, we were unsuccessful in detecting P-Y 19 and 27-Cav-2 specific signal in control, cell cycle synchronized, or treated with a combination of endothelial cell specific stimuli, such as bFGF and VEGF. Thus, our data suggest that unlike serine, tyrosine phosphorylation level of Cav-2 is very low in endothelial cells, although we cannot exclude the possibility of stimulating detectable tyrosine phosphorylation with other EC specific agonists. Alternatively, the fast turnover of tyrosine relative to serine phosphorylation may be accountable for the observed differences in detection limits between phosphoserine and tyrosine specific antibodies against Cav-2. Further studies examining the role of serine and tyrosine phosphorylation of Cav-2 in regulating cell function, including caveolae-mediated endocytosis or cell proliferation and differentiation are clearly warranted.

ACKNOWLEDGMENT

We thank Dr. Enrique Rodriquez-Booulan for AdCav-2 virus and the University of Iowa Vector Core Laboratory for AdCav-1 virus. We thank Dr. Robert Lim for his help with revising this manuscript.

REFERENCES

1. Rothberg, K. G., Heuser, J. E., Donzell, W. C., Ying, Y. S., Glenney, J. R., and Anderson, R. G. (1992) Caveolin, a protein component of caveolae membrane coats, *Cell 68*, 673−682.
2. Williams, T. M., and Lisanti, M. P. (2004) The Caveolin genes: from cell biology to medicine, *Ann. Med. 36*, 584−595.
3. Krajewska, W. M., and Maslowska, I. (2004) Caveolins: structure and function in signal transduction, *Cell. Mol. Biol. Lett. 9*, 195−220.
4. Das, K., Lewis, R. Y., Scherer, P. E., and Lisanti, M. P. (1999) The membrane-spanning domains of caveolins-1 and -2 mediate the formation of caveolin hetero-oligomers. Implications for the assembly of caveolae membranes in vivo, *J. Biol. Chem. 274*, 18721−18728.
5. Sowa, G., Pypaert, M., Fulton, D., and Sessa, W. C. (2003) The phosphorylation of caveolin-2 on serines 23 and 36 modulates caveolin-1-dependent caveolae formation, *Proc. Natl. Acad. Sci. U.S.A. 100*, 6511−6516.
6. Mora, R., Bonilha, V. L., Marmorstein, A., Scherer, P. E., Brown, D., Lisanti, M. P., and Rodriguez-Boulan, E. (1999) Caveolin-2 localizes to the golgi complex but redistributes to plasma membrane, caveolae, and rafts when co-expressed with caveolin-1, *J. Biol. Chem. 274*, 25708−25717.
7. Parolini, I., Sargiacomo, M., Galbiati, F., Rizzo, G., Grignani, F., Engelman, J. A., Okamoto, T., Ikezu, T., Scherer, P. E., Mora, R., Rodriguez-Boulan, E., Peschle, C., and Lisanti, M. P. (1999) Expression of caveolin-1 is required for the transport of caveolin-2 to the plasma membrane. Retention of caveolin-2 at the level of the golgi complex, *J. Biol. Chem. 274*, 25718−25725.
8. Drab, M., Verkade, P., Elger, M., Kasper, M., Lohn, M., Lauterbach, B., Menne, J., Lindschau, C., Mende, F., Luft, F. C., Schedl, A., Haller, H., and Kurzchalia, T. V. (2001) Loss of caveolae, vascular dysfunction, and pulmonary defects in caveolin-1 gene-disrupted mice, *Science 293*, 2449−2452.
9. Razani, B., Engelman, J. A., Wang, X. B., Schubert, W., Zhang, X. L., Marks, C. B., Macaluso, F., Russell, R. G., Li, M., Pestell, R. G., Di, Vizio, D., Hou, H., Jr., Kneitz, B., Lagaud, G., Christ, G. J., Edelmann, W., and Lisanti, M. P. (2001) Caveolin-1 null mice are viable but show evidence of hyperproliferative and vascular abnormalities, *J. Biol. Chem. 276*, 38121−38138.
10. Galbiati, F., Razani, B., and Lisanti, M. P. (2001) Emerging themes in lipid rafts and caveolae, *Cell 106*, 403−411.
11. Razani, B., Wang, X. B., Engelman, J. A., Battista, M., Lagaud, G., Zhang, X. L., Kneitz, B., Hou, H., Jr., Christ, G. J., Edelmann, W., and Lisanti, M. P. (2002) Caveolin-2-deficient mice show evidence of severe pulmonary dysfunction without disruption of caveolae, *Mol. Cell. Biol. 22*, 2329−2344.
12. Scheiffele, P., Verkade, P., Fra, A. M., Virta, H., Simons, K., and Ikonen, E. (1998) Caveolin-1 and -2 in the exocytic pathway of MDCK cells, *J. Cell Biol. 140*, 795−806.
13. Lahtinen, U., Honsho, M., Parton, R. G., Simons, K., and Verkade, P. (2003) Involvement of caveolin-2 in caveolar biogenesis in MDCK cells, *FEBS Lett. 538*, 85−88.
14. Fujimoto, T., Kogo, H., Nomura, R., and Une, T. (2000) Isoforms of caveolin-1 and caveolar structure, *J. Cell Sci.* 113 Pt *19*, 3509−3517.
15. Fujimoto, T., Kogo, H., Ishiguro, K., Tauchi, K., and Nomura, R. (2001) Caveolin-2 is targeted to lipid droplets, a new "membrane domain" in the cell, *J. Cell Biol. 152*, 1079−1085.
16. Ostermeyer, A. G., Paci, J. M., Zeng, Y., Lublin, D. M., Munro, S., and Brown, D. A. (2001) Accumulation of caveolin in the endoplasmic reticulum redirects the protein to lipid storage droplets, *J. Cell Biol. 152*, 1071−1078.
17. Sowa, G., Pypaert, M., and Sessa, W. C. (2001) Distinction between signaling mechanisms in lipid rafts vs. caveolae, *Proc. Natl. Acad. Sci. U.S.A. 98*, 14072−14077.
18. Bibby, A. C., and Litchfield, D. W. (2005) The Multiple Personalities of the Regulatory Subunit of Protein Kinase CK2: CK2 Dependent and CK2 Independent Roles Reveal a Secret Identity for CK2beta, *Int. J. Biol. Sci. 1*, 67−79.
19. Lasa-Benito, M., Marin, O., Meggio, F., and Pinna, L. A. (1996) Golgi apparatus mammary gland casein kinase: monitoring by a specific peptide substrate and definition of specificity determinants, *FEBS Lett. 382*, 149−152.
20. Olsten, M. E., Canton, D. A., Zhang, C., Walton, P. A., and Litchfield, D. W. (2004) The Pleckstrin homology domain of CK2 interacting protein-1 is required for interactions and recruitment of protein kinase CK2 to the plasma membrane, *J. Biol. Chem. 279*, 42114−42127.

21. Scherer, P. E., Lewis, R. Y., Volonte, D., Engelman, J. A., Galbiati, F., Couet, J., Kohtz, D. S., van Donselaar, E., Peters, P., and Lisanti, M. P. (1997) Cell-type and tissue-specific expression of caveolin-2. Caveolins 1 and 2 co-localize and form a stable hetero-oligomeric complex in vivo, *J. Biol. Chem. 272*, 29337−29346.
22. Lee, H., Park, D. S., Wang, X. B., Scherer, P. E., Schwartz, P. E., and Lisanti, M. P. (2002) Src-induced phosphorylation of caveolin-2 on tyrosine 19. Phospho-caveolin-2 (Tyr(P)19) is localized near focal adhesions, remains associated with lipid rafts/caveolae, but no longer forms a high molecular mass hetero-oligomer with caveolin-1, *J. Biol. Chem. 277*, 34556−34567.
23. Wang, X. B., Lee, H., Capozza, F., Marmon, S., Sotgia, F., Brooks, J. W., Campos-Gonzalez, R., and Lisanti, M. P. (2004) Tyrosine phosphorylation of caveolin-2 at residue 27: differences in the spatial and temporal behavior of phospho-Cav-2 (pY19 and pY27), *Biochemistry 43*, 13694−13706.

BI701709S